A Strategy for Source-Seeking applied for Inspection of Belt Conveyor Rollers

Henrique D. Faria , Fernando Lizarralde and Ramon R. Costa

Abstract— In this paper, a sliding mode control using a periodic search function strategy is used to drive a robot to the origin of a stationary sound source in an industrial inspection scenario. The robotic system is composed of a mobile base equipped with a manipulator arm. A extremum-seeking controller is designed to drive the cartesian position of the manipulator to the maximum of an unknown field that represents the source of the sound emitted by a damaged roller of a belt conveyor idler. Simulation results considering the kinematic model of the robot ROSI are presented with satisfactory results.

I. INTRODUCTION

Conveyor structures require permanent inspection and maintenance. Being the most common means used to transport bulk material in the mineral industry [1], and having extensions ranging from a dozen meters to several dozens of kilometers [2]. In recent years the inspection tasks have been subject of many researches aiming to modify this process to use autonomous robots instead of human inspectors [3] [4] [2] and [5]. Some of the potential benefits expected to be brought by this transformation are the reduction of exposure of workers to harsh environment, as well as to enable more standardized inspections, and less dependent on human individual senses [3], which would potentially lead to a better maintenance and reduced costs associated with unpredicted plant stops.

In the context of those structures, several works address the diagnostics of drive units using vibration analysis, infrared thermography, or temperature. Since the conveyor belt is the most expensive component in the structure, various nondestructive techniques, such as image analysis, laser scanning, and magnetic field measurement, have been applied to diagnose the damage [5]. Rolling element bearings are used in electric motors, gearboxes, pulleys, and, on a massive scale, in idler rollers, and vibration signals are the most commonly used method for fault detection, while acoustic emission signals are also possible.

The use of sound signals for fault detection and diagnostics in idler bearings have been studied by [6], [7], [8], [2] and [5]. In [6] Wavelet Transform and Back-Propagation are used to automatically detect and identify faults in Belt Conveyor, where a fault characteristic information can be obtained by

Fig. 1. Robotic inspection of a belt conveyor.

adding the energy of each band after the wavelet transform of the faulty sound. In [8], the Mel-Frequency Cepstral Coefficients and Gradient Boost Decision Tree are used in feature extraction and classification of faults on belt conveyor (BC) idler rolls.

In [5], the authors show that damage detection in belt conveyor bearings using acoustic signals is possible using a mobile robot, even in the presence of a significant amount of background noise and the influence of the sound disturbance due to the belt joint. In [2], the authors describe a method for detection of conveyor rollers failure based on an offline processing of acoustic signal acquired using a legged robot to autonomously inspect about 100m of operating belt conveyor.

Once the robot has detected the existence of a damaged roller by regularly analyzing the ambient sound, an important challenge is to seek the source of that sound, since it would be too costly to individually inspect each roller of each idler in a section of the conveyor. Seeking the source of a measurable phenomenon whose distribution is unknown has important applications, like locating the source of nuclear radiation and the leakage of a contaminant in the ocean. In [9] source seeking is considered as the problem of maximizing a convex potential induced by the source.

In [10], [11] a sliding mode control strategy is used to guide an autonomous vehicle towards the source of a considered phenomenon to determine its position.

Extremum-Seeking Control (ESC) is a technique whose objective is to design a controller capable of steer the system

output to follow a non-predetermined optimal operating point [12] without prior knowledge of the model. In [13], the authors divide the different methods for ESC, roughly in three categories:

- The most well known, presented in [14] is based on periodic perturbation signals, or *dithers*.
- The method presented in [15] and [16] for extremal control uses monitoring functions and sliding modes, where the monitoring function is used to overcame the lack of knowledge about the control direction.
- In [12], the authors propose a strategy for multivariable extremal control based on periodic switching function and sliding mode, where a cyclic search is introduced to reduce the multivariable problem to a sequence of scalar subproblems.

In this paper, the authors propose the application of the extremum-seeking control strategy based on periodic switching function [13], to steer a mobile manipulator towards the close neighborhood of a damaged roller, the assumed noise source, so that further inspection can be done using the set of sensors tied to its end-effector. Without loss of generality, this work is developed considering ROSI, a mobile robot designed for industrial applications on poorly structured environments [17], [18]. It is composed of a four wheels skid-steered mobile base with four tracked flippers that allows the robot to overcame obstacles, and a 7-DoF manipulator arm. In Section 2 we present the problem formulation, the control strategy is described in Section 3. Sections 4 and 5 present simulation results and the conclusion, respectively.

II. PRELIMINARIES

An important operational scenario consists of a conveyor structure running through a large distance with lots of idler rollers supporting the belt, as seen in Figure 1.

In [18], a novel conceptual robotic inspection procedure is proposed to address the robotic inspection. Based on such procedures, it is considered here a situation in which the robot detects some sound anomaly in its surroundings. Once detected, the robot should move by the side of the conveyor searching for the best position to perform further inspection with other sensors, thus avoiding the hassle of individually analyze each idlers' components.

As usual in mobile manipulation [19], we break the procedure in two stages. In the first stage, the vehicle should be driven to the closest point, to the source, that can be reached along side the conveyor. As shown in Figure 2, it may not be possible to identify, just by this procedure, which of the rollers composing the idler is damaged. In the second stage, the same control strategy is used to move the sensor pack in the manipulator end-effector tip to a position even closer. Although not considered here, [20] presents some strategies that could be used to avoid unintentional contact with the structure.

Assumption 1: The damaged roller's sound emission contains a set of characteristics that differentiate it from non-damaged rollers, and these characteristics are stationary and can be isolated by either filtering, machine learning or other

Fig. 2. From the robot position, any of the rollers could be the source of the noisy sound.

signal processing technique as those shown in [21] [22] [7] [8] [2] and [5], and can be used to produce a quantifiable measurement whose maximum coincide with the position of the damaged roller.

A. Robot Model

Let $\mathscr{F}_g$ be the inertial frame, e.g. at the beginning of a conveyor structure, $\mathscr{F}_r$ be a frame fixed in the mobile base chassi, $\mathscr{F}_b$ be a frame fixed at the base of the arm, and $\mathscr{F}_e$ a frame fixed at the end-effector. From [19] we have that the configuration of the end-effector with respect to the frame $\mathscr{F}_g$ can be described by the homogeneous transformation:

$$T_{ge}(q,\theta) = T_{gr}(q)T_{rb}T_{be}(\theta) \in \mathbb{SE}(3), \tag{1}$$

where $q = (p_{xr}, p_{yr}, \phi_{zr})$ is the planar configuration of the mobile base, $\theta \in \mathbb{R}^n$ is the set of joint angular positions of the n-DoF manipulator arm, and the transformation

$$T_{gr}(q) = \begin{bmatrix} \cos(\phi_{zr}) & -\sin(\phi_{zr}) & 0 & p_{xr} \\ \sin(\phi_{zr}) & \cos(\phi_{zr}) & 0 & p_{yr} \\ 0 & 0 & 1 & p_{zr} \\ 0 & 0 & 0 & 1 \end{bmatrix}, \tag{2}$$

describes the configuration of frame $\mathscr{F}_r$ with respect to the inertial frame $\mathscr{F}_g$, where p_{zr} represents the height of $\mathscr{F}_r$ with respect to $\mathscr{F}_g$ and, without loss of generality, is assumed to be constant here.

The transformation T_{rb} is a fixed offset distance of frame $\mathscr{F}_b$ from $\mathscr{F}_r$, and the the transformation $T_{be}(\theta)$ is the forward kinematics of the manipulator, given by

$$T_{be}(\theta) = \begin{bmatrix} R_{be} & p_{be} \\ 0 & 1 \end{bmatrix}, \tag{3}$$

where $p_{be} \in \mathbb{R}^3$ is the end-effector position with respect to the robot manipulator base frame $\mathscr{F}_b$, and $R_{be} \in \mathbb{SO}(3)$ is the rotation matrix of the tool frame $\mathscr{F}_e$ with respect to the base frame $\mathscr{F}_b$.

As in [3], we consider $[v_r\, \omega_r]^\top$ the input commands to the mobile base, such that

$$\begin{bmatrix} \dot{p}_{xr} \\ \dot{p}_{yr} \\ \dot{\phi}_{zr} \end{bmatrix} = \begin{bmatrix} \cos(\phi_{zr}) & 0 \\ \sin(\phi_{zr}) & 0 \\ 0 & 1 \end{bmatrix} \begin{bmatrix} v_r \\ \omega_r \end{bmatrix}, \tag{4}$$

The end-effector linear velocity $\dot{p}_{be}$ expressed in the base frame $\mathscr{F}_b$, is related to the joint velocity $\dot{\theta} \in \mathbb{R}^n$ by the differential kinematics equation as [23]:

$$\dot{p}_{be} = J_p(\theta)\dot{\theta}, \tag{5}$$

where $J_p(\theta) \in \mathbb{R}^{3 \times n}$ is the position manipulator jacobian, which can be computed analytically as $J_p(\theta) = (\partial p_{be}(\theta)/\partial \theta)$.

Now, considering the kinematic control approach, the manipulator motion can be simply described by:

$$\dot{\theta}_i = u_i, \quad i = 1, ..., n, \tag{6}$$

where $\dot{\theta}_i$ are the angular velocity of the i-th joint and u_i is the velocity control signal applied to the i-th joint motor drive. This assumption can be applied to most commercial manipulators with high gear reduction ratios and/or when the manipulator motions are performed with low velocities and accelerations. In such cases, the effects of nonlinear coupling terms of the manipulator dynamics can be neglected and the kinematic control approach ensures a satisfactory performance for the feedback system [23]. Thus, replacing (6) into (5), we obtain the following control system:

$$\dot{p}_{be} = J_p(\theta)u, \tag{7}$$

A cartesian control signal $v_k(t)$ can be transformed into joint control signals $u \in \mathbb{R}^n$ by using a simple inverse kinematics algorithm:

$$u = J_p^{\dagger}(\theta)v_k, \tag{8}$$

where $J_p^{\dagger} = J_p^{\top}(J_pJ_p^{\top})^{-1}$ is the right pseudo-inverse matrix of $J_p(\theta)$, which is assumed to be full row rank. Therefore, substituting (8) into (7), the kinematic control system (Fig. 3) is given by

$$\dot{p}_{be} = v_k, \tag{9}$$

and naturally $v_k \in \mathbb{R}^3$ is designed to control the position of the manipulator end-effector. Notice that, the relationship (9) is valid if, and only if, the following two assumptions hold:

Assumption 2: The manipulator kinematics is known exactly.

Assumption 3: The control law $v_k(t)$ does not drive the robot manipulator to singular configurations.
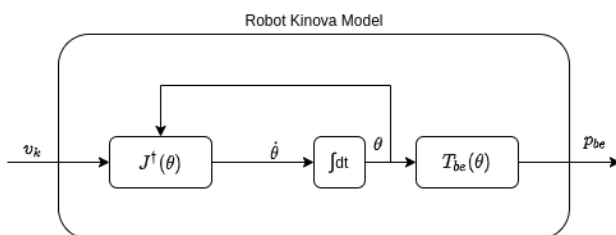
Robot Kinova Model

Fig. 3. Block diagram of the kinematic control system

B. Field Model Characteristics

Let the target sound emission be represented as the non-linear field in the three dimensional region $D \subset \mathbb{R}^3$

$$h_e = \Phi(x) \tag{10}$$

where $h_e \in \mathbb{R}$ represents the instantaneous measurement result in the cartesian position $x \in \mathbb{R}^3$ relative to the frame $\mathscr{F}_g$, mapped by the unknown mapping function $\Phi(x) : D \to \mathbb{R}$. Here, the time dependency is omitted since the target noise is assumed to be stationary, so the measurement result h depends only on the robot position.

Assumption 4: The mapping function $\Phi(x)$ is continuously differentiable in $D \in \mathbb{R}^3$.

Assumption 5: There exists $x^* \in \mathbb{R}^3$ such that $h_e^* = \Phi(x^*)$ is the only maximum in $\Phi(x)$.

Assumption 6: The function $\Phi(x) : D \to \mathbb{R}$ is radially unbounded in $\mathbb{R}^3$, which guarantees that if $|h_e|$ is bounded, then $\|x\|$ must be bounded.

III. PROBLEM FORMULATION

The objective of the *source-seeking control strategy* is to find x^* that maximizes the measurement h_e. The task is divided in two stages, as mentioned in section II.

Considering that the conveyor is a straight line, and that the frame $\mathscr{F}_g$ is fixed with its x-axis parallel to the structure and z-axis pointing upwards. In Stage 1 the control strategy should be capable of steering the robot to the closest neighborhood of the damaged roller using the characteristic noise emission as input, i.e. to generate the necessary input values $[v_r, \omega_r]^{\top}$ such that

$$q_{y\phi}(t) \to q_{y\phi}^* \quad \text{when} \quad t \to t_{f1}, \tag{11}$$

where $q_{y\phi}(t) = (x(t), y_0, \phi_0)$ is the base configuration with $y = y_0$ and $\phi = \phi_0$ kept constant during the search, and $q_{y\phi}^* = (x^*, y_0, \phi_0)$ is the configuration that maximizes the field measurement $h_e = \Phi(p_{be})$ along the line $(x(t), y_0, \phi_0)$.

In Stage 2, the manipulator arm should move from its *resting*, θ_{rst}, towards a *ready*, θ_{rdy}, configuration to start another search inside the manipulator workspace. During this search, the controller should provide the needed input signal v_k to drive the end-effector from $T_{ge}(q_{y\phi}^*, \theta_{rdy})$ to the configuration $T_{ge}(q_{y\phi}^*, \theta^*)$.

Although the scenario described in II doesn't cover all possible conveyor belt structure environments existent, not even all environments in which the robots is expected to be used, it is still a very important scenario due to the large distances covered by this specific subset. Considering that a small conveyor belt of 150 meters has nearly 450 carrying rollers and 50 return rollers [1], it would be very inefficient to individually inspect each bearing from each roller in a kilometer scaled structure.

IV. EXTREMUM-SEEKING CONTROLLER

As discussed in section III, for both the robot base and the manipulator end-effector, a desired velocity can be used as input to a kinematic controller in order to actuate on the cartesian positions.

According to [13] the extremal control can be reformulated as tracking problem with unknown control trajectory. Thus, it is necessary to find a feedback control law v_k such that, from any initial condition, the system converges to a close neighborhood of h^*. Figure 4 shows the extremum-seeking control strategy adopted.

Since $\Phi(x)$ is unknown we define the tracking error as:

$$e(t) = h_e(p_{be}(t)) - h_m(t) \tag{12}$$

where $e \in \mathbb{R}$, h_e is measurement at the end-effector position, $h_m \in \mathbb{R}$ is a monotonically increasing function, whose dynamic is given by:

$$\dot{h}_m = a_m, \tag{13}$$

$a_m \in \mathbb{R}^+$, and $h_m(0) = h_e(0)$. To avoid an unbounded reference signal $h_m(t)$ in the controller, it is possible to impose an upper bounding of h^* using a saturation function without affecting the extremum controller performance.

As shown in figure 4, the control law given by:

$$u(t) = \rho(t)\sigma(t)sgn\left[\sin\left(\frac{\pi}{\varepsilon}s(t)\right)\right] \tag{14}$$

where $\rho(t)$ is the modulation function, $\sigma(t)$ is the cyclic search, $\varepsilon \in \mathbb{R}^+$ is a constant and $s(t) \in \mathbb{R}$ is defined as shown below:

$$s(t) = e(t) + \lambda \int_0^t sgn(e(\tau))d\tau \tag{15}$$

where $\lambda \in \mathbb{R}^+$.

The modulation function $\rho(t)$ is defined as:

$$\rho(t) = \bar{d}_s + \gamma \tag{16}$$

where γ is a positive small constant, and $\bar{d}_s$ is the constant bounding value of the perturbation d_s defined as

$$\bar{d}_s := L_h^{-1}(a_m - \lambda) \geq |d_s| \tag{17}$$

The cyclic search function is designed such that the searching direction is changed periodically. Consider a time interval $T = [\tau_l, \tau_u)$, and the period $\tau = \tau_u - \tau_l$. The set of time instants $\tau_1, \tau_2, ..., \tau_n \in T$ such that $\tau_l = \tau_1 < \tau_2 < ... \tau_n < \tau_{n+1} = \tau_u$, and $\Delta \tau_i = [\tau_i, \tau_{i+1}) \forall i \in \{1, 2, ..., n\}$ are subintervals, thus subset, of T.

Let $\sigma(t)$ be a function with period τ, i.e. $\sigma(t + \tau) = \sigma(t)$, such that

$$\sigma(t) = \begin{bmatrix} \sigma_{\tau_1}(t) \\ \sigma_{\tau_2}(t) \\ ... \\ \sigma_{\tau_n}(t) \end{bmatrix} \tag{18}$$

where $\sigma_{\tau_i}(t)$ are square waves of period τ and duty cycle defined by $100\frac{\tau_i}{\tau}\%, \forall i \in 1, 2, ..., n$.

Given the period τ, an index $\kappa = 1, 2, ..., \infty$ is attributed to each cycle. For κ-th cycle, the directional extremum can occur for the i-th search inside the cycle. Such extremum is denoted $h_i^*(\kappa) = \Phi(x^*(\kappa))$, where $x(t) \in \mathbb{R}^3$ is a position with respect to $\mathscr{F}_g$ and $x^*(\kappa)$ is a maximum point in the i-th search direction of the κ-th cycle.

When the system approaches a global or a directional maximum, the controller gains are too small to guarantee the output tracking in sliding mode. These regions of low controllability are defined as $D_\Delta := \{x : ||x - x^*|| < \frac{\Delta}{2}\}$, and $D(\kappa_i)_{\Delta_i} := \{x : ||x_i(\kappa_i) - x_i^*(\kappa_i)|| < \frac{\Delta_i}{2}, x_j(\kappa_i) = constant, \forall j \neq i\}$ for each i-th directional search of the κ-th cycle, indexed as κ_i. The following theorem [13] summarize the convergency properties of the proposed extremum seeking controller :

Theorem 1: [13] Consider the system (9)–(10), the control law (14)-(15), the reference trajectory (13) and the modulating function (16)-(17). Then, under assumptions 4-6, the following properties hold: (i) the region D_Δ is globally attractive, being reached in finite time; and (ii) for L_h sufficiently small, the oscillations around the maximum value h_e^* of h_e can be made of order $O(\varepsilon^2)$. Since the signal h_m can be saturated in (13), all signal in closed loop are uniformly bounded.

V. SIMULATION RESULTS

The simulations is divided in two parts. The first representing the initial search in x direction performed with the manipulator in *rest position*. The second part uses the mobile base final position, from part 1, as initial position for the manipulator base frame. The controller parameters for both simulations can be seen in table II and the Denavit-Hartemberg parameters of the manipulator used are shown in table I.

i	θ_i	d_i	a_i	α_i
1	θ_1	$-(0.1564 + 0.1284)$	0.0	$\pi/2$
2	θ_2	0.0	0.0	$\pi/2$
3	θ_3	$-(0.2104 + 0.2104)$	0.0	$\pi/2$
4	θ_4	0.0	0.0	$\pi/2$
5	θ_5	$-(0.2084 + 0.1059)$	0.0	$\pi/2$
6	θ_6	0.0	0.0	$\pi/2$
7	θ_7	0.0	0.0	π

TABLE I

DENAVIT-HARTENBERG PARAMETERS

The unknown field $\Phi(x)$ is represented as the Gaussian distribution as shown bellow

$$\Phi(x) = \frac{1}{\sqrt{2\pi\sigma^2}}e^{-\frac{(x-\mu_x)^2+(y-\mu_y)^2+(z-\mu_z)^2}{2\sigma^2}} \tag{19}$$

where $x = [p_x \quad p_y \quad p_z]^T$, $\sigma = 4$ and $\mu = [7 \quad 1.5 \quad 1]^T$.

The system is simulated in Simulink and MATLAB 2021a, with the addition of Robotics Toolbox [24], using fixed timestep size $st = 0.0001$.

The gain vector a_{gain} is added to the simulation model multiplying element-wise the cyclic search signal $\sigma(t)$ in such a way that its elements are either 0 or 1, thus allowing to restrict the cyclic search only in the x-direction by choosing its other components as zeros in the simulation of Stage 1 and ones in Stage 2. The controller parameters are tunned to comply with the constrains in the joint velocities imposed by the vehicle and manipulator specifications.
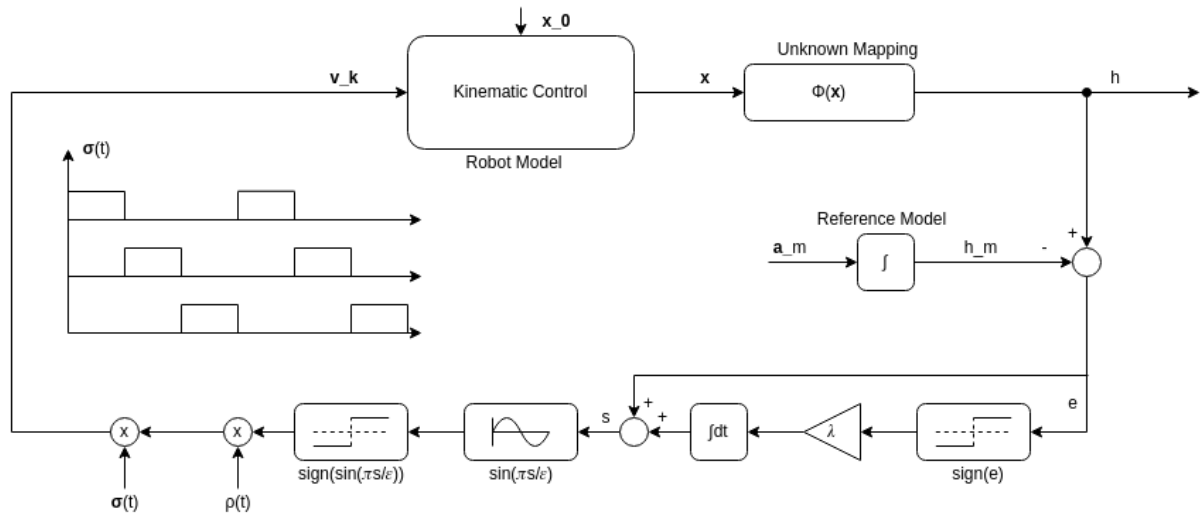
Fig. 4. Block diagram of the source-seeking control strategy

In Stage 1 results the robot base is driven from the initial position to the point $\Phi(6.9956, 1.0, 0.5)$. Note that the point $(x^*, 1.0, 0.5) = (7, 1.0, 0.5)$ is the point where the field $\Phi(x^*, 1.0, 0.5)$ is maximum in the segment $(x(t), 1.0, 0.5)$. See figure 5.

In Stage 2 the simulations are run using the kinematics model of the manipulator, in the results shown in figure 6 it is possible to see the search in the different directions taking place each cycle. In figure 7 the overall simulation results are shown as a composition of the data from first and second Stages.

Parameter	Stage 1: Vehicle	Stage 2: Manipulator
$\mathbf{x}_0 = (x_0, y_0, z_0)$	$(1.0, 1.0, 0.5)$	$(6.9956, 1.0, 0.5)^\star$
a_m	0.004	0.0015
h_{m0}	$\Phi(1.0, 1.0, 0.5)$	$\Phi(6.9956, 1.0, 0.5)$
λ	2.8	0.2
ε	0.001	0.00015
$\bar{d}_s$	4.9	0.5
γ	0.1	0.5
τ	1.5	0.15
$\mathbf{a}_{gain}$	$(1.0, 0.0, 0.0)$	$(1.0, 1.0, 1.0)$

TABLE II

SIMULATION PARAMETERS. $\star$: INHERITED FROM SIMULATION 1.

VI. CONCLUSION

ionIn this work, the source seeking problem is applied in the context of industrial inspection performed by a mobile robot. A Gaussian function is used as an hypothetical model of the output of sound acquisition and processing system, used to identify the location of a damaged roller.

The Extremum-Seeking controller based on cyclic search function proposed in [13] is applied, in simulation environment, to drive a robot model to the close neighborhood of the maximum point of a field used to represent the processed measurement of the noisy sound emitted by the damaged roller. As future work, it is possible to point out a few topics:

- the development of a field function that better models the source;
- implement the controller and one of the pre-processing algorithms mentioned in III in a mobile robot and run a simplified real world experiment with only one damaged roller;
- the controller used in this work was developed assuming a single maximum point, since this condition might not be true in the real world application, it would be important to evaluate whether the results are extensible a scenario with multiple extrema, and
- study other classes of search functions.

REFERENCES

[1] R. Nascimento, R. Carvalho, S. Delabrida, A. Bianchi, R. A. R. Oliveira, and L. G. U. Garcia, "An integrated inspection system for belt conveyor rollers," in *Proc. 19th Int. Conf. Enterprise Inf. Sys. (ICEIS)*, vol. 2, 2017, pp. 190–200.

[2] A. Skoczylas, P. Stefaniak, S. Anufriiev, and B. Jachnik, "Belt conveyors rollers diagnostics based on acoustic signal collected using autonomous legged inspection robot," *Applied Sciences*, vol. 11, no. 5, p. 2299, 2021.

[3] G. Garcia, F. Rocha, M. Torre, W. Serrantola, F. Lizarralde, A. Franca, G. Pessin, and G. Freitas, "ROSI: A novel robotic method for belt conveyor structures inspection," in *19th International Conference on Advanced Robotics (ICAR)*, 2019, pp. 326–331.

[4] H. Staab, E. Botelho, D. T. Lasko, H. Shah, W. Eakins, and U. Richter, "A robotic vehicle system for conveyor inspection in mining," in *2019 IEEE Int. Conference on Mechatronics (ICM)*, 2019, pp. 352–357.

[5] H. Shiri, J. Wodecki, B. Zietek, and R. Zimroz, "Inspection robotic UGV platform and the procedure for an acoustic signal-based fault detection in belt conveyor idler," *Energies*, vol. 14, no. 22, p. 7646, 2021.

[6] X. P. Jiang and G. Q. Cao, "Belt conveyor roller fault audio detection based on the wavelet neural network," in *11th International Conference on Natural Computation (ICNC)*. IEEE, 2015, pp. 954–958.

[7] M. Yang, W. Zhou, and T. Song, "Audio-based fault diagnosis for belt conveyor rollers," *Neurocomputing*, vol. 397, pp. 447–456, 2020.

[8] X. Liu, D. Pei, G. Lodewijks, Z. Zhao, and J. Mei, "Acoustic signal based fault detection on belt conveyor idlers using machine learning," *Advanced Powder Technology*, vol. 31, no. 7, pp. 2689–2698, 2020.

[9] B. A. Angélico, L. F. Chamon, S. Paternain, A. Ribeiro, and G. J. Pappas, "Source seeking in unknown environments with convex obstacles," in *American Control Conference (ACC)*, 2021, pp. 5055–5061.
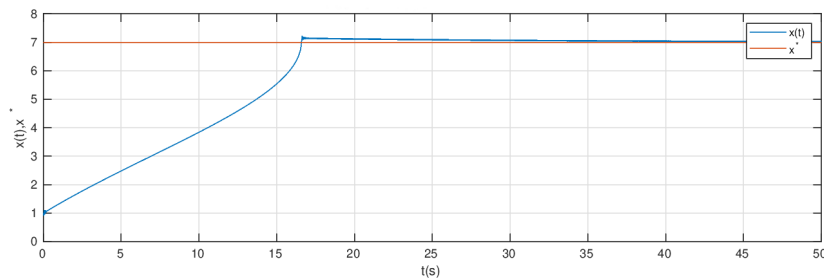
Fig. 5.   Mobile base position in simulation part 1, in blue. The value that maximizes the field in the search direction is shown in red.
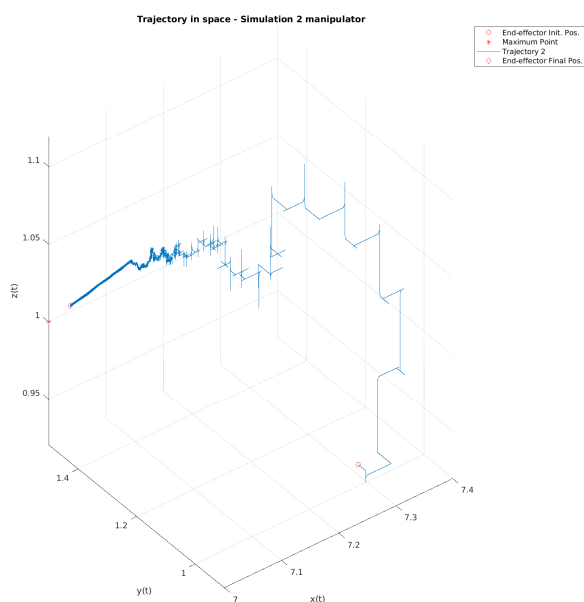

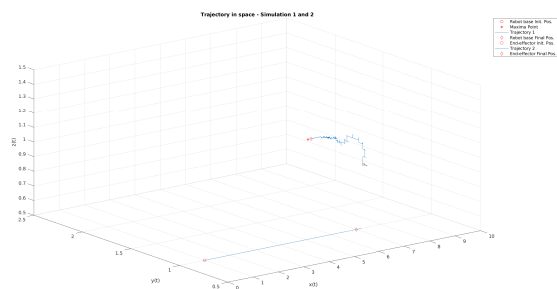Fig. 6.   Robot end-effector trajectory simulated using robot kinematic model

Fig. 7.   Robot end-effector trajectory composing data from simulation 1 and 2 using robot kinematic model

[10] C. Mellucci, P. P. Menon, C. Edwards, and P. Challenor, "Source seeking using a single autonomous vehicle," in *American Control Conference (ACC)*, 2016, pp. 6441–6446.

[11] C. Mellucci, P. P. Menon, C. Edwards, and P. G. Challenor, "Environmental feature exploration with a single autonomous vehicle," *IEEE Transactions on Control Systems Technology*, vol. 28, no. 4, pp. 1349–1362, 2020.

[12] Y. B. Salamah and Ü. Özgüner, "Sliding mode multivariable extremum seeking control with application to wind farm power optimization," in *American Control Conference (ACC)*, 2018, pp. 5321–5326.

[13] N. O. Aminde, T. R. Oliveira, and L. Hsu, "Controle multivariável para busca extremal cíclica usando modos deslizantes e função de chaveamento periódica," in *Congresso Brasileiro de Automática (CBA)*, 2020.

[14] M. Krstić and H.-H. Wang, "Stability of extremum seeking feedback for general nonlinear dynamic systems," *Automatica*, vol. 36, no. 4, pp. 595–601, 2000.

[15] N. O. Aminde, T. R. Oliveira, and L. Hsu, "Global output-feedback extremum seeking control via monitoring functions," in *52nd IEEE Conference on Decision and Control*, 2013, pp. 1031–1036.

[16] T. R. Oliveira, N. O. Aminde, and L. Hsu, "Monitoring function based extremum seeking control for uncertain relative degrees with light source seeking experiments," in *53rd IEEE Conference on Decision and Control*, 2014, pp. 3456–3462.

[17] H. D. Faria, F. Lizarralde, R. R. Costa, R. H. Andrade, T. H. Silva, R. F. Pereira, E. S. Barbosa, F. Rocha, A. Franca, G. M. Freitas *et al.*, "ROSI: a mobile robot for inspection of belt conveyor," *IFAC-PapersOnLine*, vol. 53, no. 2, pp. 10 031–10 036, 2020.

[18] F. Rocha, G. Garcia, R. F. Pereira, H. D. Faria, T. H. Silva, R. H. Andrade, E. S. Barbosa, A. Almeida, E. Cruz, W. Andrade *et al.*, "ROSI: A robotic system for harsh outdoor industrial inspection-system design and applications," *Journal of Intelligent & Robotic Systems*, vol. 103, no. 2, pp. 1–22, 2021.

[19] K. M. Lynch and F. C. Park, *Modern Robotics*.   Cambridge University Press, 2017.

[20] F. Coutinho, I. Novais, and F. Lizarralde, "Controle com restrição de manipulador móvel para tarefas de inspeção em ambiente industrial," in *Anais do 24º Congresso Brasileiro de Automática (CBA)*, Fortaleza (CE), 2022.

[21] J. Grebenik, Y. Zhang, C. Bingham, and S. Srivastava, "Roller element bearing acoustic fault detection using smartphone and consumer microphones comparing with vibration techniques," in *17th Int. Conference on Mechatronics Mechatronika*, 2016, pp. 1–7.

[22] P. Rzeszucinski, M. Orman, C. T. Pinto, A. Tkaczyk, and M. Sulowicz, "Bearing health diagnosed with a mobile phone: Acoustic signal measurements can be used to test for structural faults in motors," *IEEE Industry Applications Magazine*, vol. 24, no. 4, pp. 17–23, 2018.

[23] B. Siciliano, L. Sciavicco, L. Villani, and G. Oriolo, *Robotics: Modelling, Planning and Control*.   Springer-Verlag London, 2009.

[24] P. Corke, *Robotics, Vision and Control*.   Springer, 2011.